3P4-2

Origin of the broadband noise of acoustic emission based on the dynamic behavior of a single bubble

Hyang-Bok Lee[1†], and Pak-Kon Choi[2]
([1]Japan Women's Univ.; [2]Meiji Univ.)

1. Introduction

Acoustic emission (AE) has been utilized to monitor to the strength of acoustic cavitation bubbles in liquid subjected to ultrasonic irradiation.

The phenomena associated with cavitating bubbles includes fragmentation, coalescence, non-spherical oscillations, which contribute to the generation of harmonics, sub-harmonics, ultra-harmonics, and broadband noise in the pressure spectrum of hydrophone signals. In particular, the broadband noise has been employed as a measure of cavitation intensity, although the origin of broadband noise has not been definitively established because of intricate bubble dynamics [1, 2]. This study investigates broadband noise from a dancing bubble observed a single bubble sonoluminescence (SBSL). AE measurements were performed simultaneously with the observation of bubble movement using a high-speed camera to explore the origin of the broadband noise associated with bubble dynamics.

2. Methods

Figure 1 shows the experimental setup. A rectangular quartz glass cell with 65 mm in width, 65 mm in depth and 90 mm in height serves as an acoustic resonator. A sandwich-type piezoelectric transducer with a fundamental frequency of 28 kHz was glued to the bottom of the cell. The sample liquid was deionized water, which was degassed until the dissolved oxygen content reached 1.5 mg/L. A continuous sinusoidal signal with a frequency of 28.4 kHz supplied by a function generator (Tektronix, AFG 3022) was amplified using a power amplifier (NF Design 4005, gain 37dB), impedance matched with a transformer, and then applied to the transducer. Acoustic signals were detected using a homemade hydrophone of 4 mm in diameter, which employs a 1-MHz PZT sensor (1.87 mV/atm). The hydrophone was located approximately 15 mm diagonally above the bubble where the bubble stability was not disturbed. The liquid surface was covered with a 0.1 mm thick PET film with a hole for the hydrophone. The SBSL intensity was measured using a photomultiplier (Hamamatsu Photonics H7422-01) and observed using an oscilloscope (R&S RTM3004, 5G Sa/s). The AE power spectra were analyzed with a spectrum analyzer (Tektronix RSA306B). To correlate with the AE measurements, high-speed photography of cavitating bubble was simultaneously captured using a high-speed video camera (Photron, SA3) with a frame speed of 30 kfps with an exposure time of 2 μs.

E-mail: †leeh@fc.jwu.ac.jp

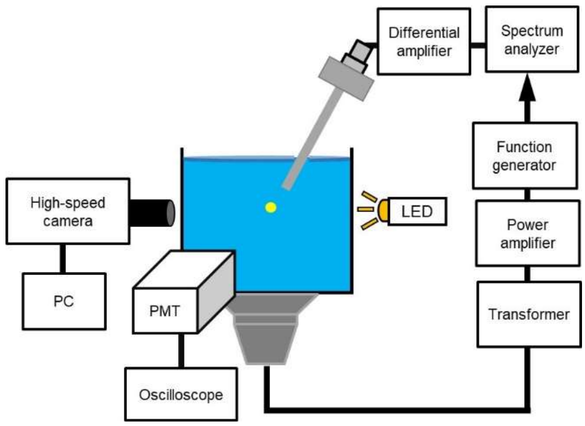

Fig. 1 Schematic diagram of the experimental setup.

3. Results and discussion

The SBSL intensity was measured as a function of the output voltage, as shown in Fig. 2. At an output voltage of 440 mV$_{pp}$, the bubble exhibited frequently dancing which resulted from bubble fragmentation and coalescence. Increasing the output voltage to 460 mV$_{pp}$ resulted in the bubble becoming spatially stable during occasional. Further

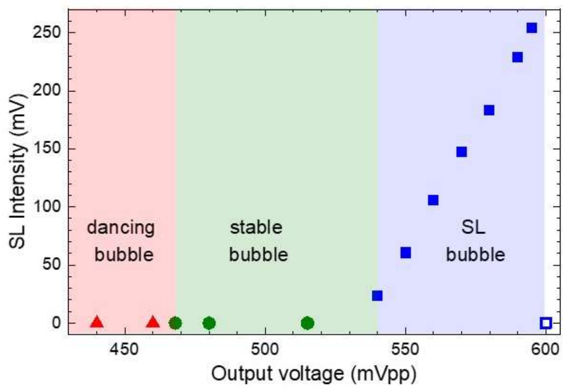

Fig. 2 Intensity of SBSL as a function of the output voltage.

increase in the output voltage to 468 mV_{pp} resulted in the spatial stability of bubble. Bluish-white light emission was observed at 540 mV_{pp} and the intensity of the SBSL increased with an increase in the output voltage. At 600 mV_{pp}, the bubble disappeared completely. We performed AE measurements for frequently-dancing bubble and the SBSL bubble. Simultaneously, high-speed photography of the bubble was captured.

Figures 3 (a), (b), and (c) show the averaged spectrum of the SBSL bubble, and the spectrum and spectrogram of the frequently-dancing bubble, respectively. A comparison of (a) with (b) shows that only fundamental (f_0) and harmonics (nf_0) were observed in the SBSL bubble, whereas the broadband noise was prominent in the frequently-dancing bubble. Figure 3 (c) shows the spectrogram of the frequently-dancing bubble in the range of 0 to 1 MHz over 14.8 ms. Five broadband noises were measured within this time frame. Comparison between 1 and 5 reveals that the former has a shorter duration for broadband noise and a narrower frequency range.

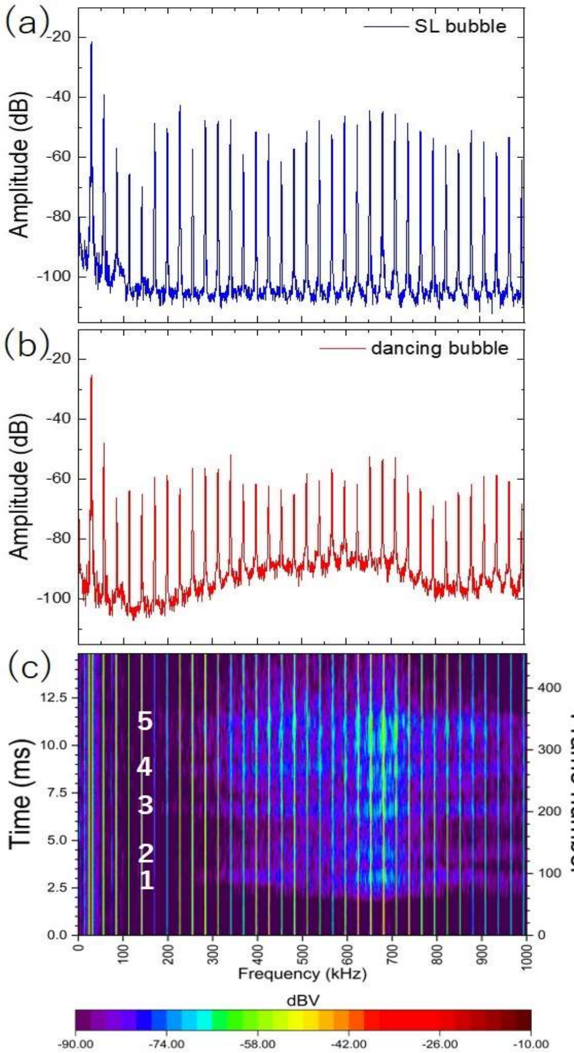

Fig. 3 Averaged spectrum for the SBSL bubble (a), and the spectrum (b) and spectrogram (c) for the frequently-dancing bubble. Blue horizontal areas indicate the broadband noise. The frame number in the right axis is corresponding to the bubble images in Fig. 4.

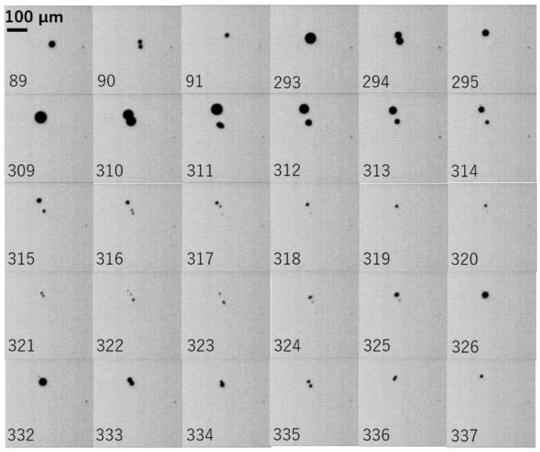

Fig. 4 Selected images of high speed photography captured for frequently-dancing bubble. The number in the images denotes a frame number and the frame interval is 33 μs.

Figure. 4 shows selected images of high-seed photography captured from the frequently-dancing bubble captured at the same time as the spectrogram shown in Fig. 3 (c). Numbers in the images denote frame number and the frame interval is 33 μs. In frame 90, the bubble fragmented into two and existed in close contact. Subsequently, the two bubbles coalesced in frame 91. Throughout frame 293 to 337, the bubble fragmented and coalesced multiple time in succession. Furthermore, the bubble separated by a distance equal to the maximum diameter in frame 311, also fragmented into three bubbles in frame 316 and 322.

When more severe fragmentation and coalescence occurred, broadband noise was measured over a wide frequency range, suggesting that broadband noise was associated with bubble fragmentation and coalescence. The bubble shape oscillation increase caused the emission of daughter bubbles and bubble fragments, resulting in the appearance of dancing bubbles [3].

Further research is necessary to understand the impact of shape oscillation on broadband noise. It is essential to analyze the two processes individually, during the instances of fragmentation and coalescence.

References

1) W. Lauterborn and T. Kurz, Rep. Prog. Phys. **73,** 106501 (2010).
2) K. Yasui, Ultrason. Sonochem. **93,** 106276 (2001).
3) Y. Tian et al. J. Acoust. Soc. Am. **100,** 3976 (1996).